Carbohydrate Polymers 123 (2015) 369–380

Contents lists available at ScienceDirect

Carbohydrate Polymers

journal homepage: www.elsevier.com/locate/carbpol

Hybrid nanosystems based on natural polymers as protein carriers for respiratory delivery: Stability and toxicological evaluation

Susana Rodrigues[a], Clara Cordeiro[b,c,d], Begoña Seijo[e], Carmen Remuñán-López[e], Ana Grenha[a,*]

[a] CBME – Centre for Molecular and Structural Biomedicine/IBB – Institute for Biotechnology and Bioengineering, University of Algarve, Faculty of Sciences and Technology, Campus de Gambelas, 8005-139 Faro, Portugal
[b] Faculty of Sciences and Technology, University of Algarve, Campus de Gambelas, 8005-139 Faro, Portugal
[c] CEAUL – Center of Statistics and Applications, Faculty of Sciences, University of Lisbon, Campo Grande, 1749-016 Lisboa, Portugal
[d] CESUAlg – Centre for Research and Development in Health, University of Algarve, Portugal
[e] NanoBioFar Group, Department of Pharmacy and Pharmaceutical Technology, Faculty of Pharmacy, University of Santiago de Compostela, Campus Vida, 15782 Santiago de Compostela, Spain

ARTICLE INFO

Article history:
Received 18 August 2014
Received in revised form
27 November 2014
Accepted 21 January 2015
Available online 3 February 2015

Keywords:
Biocompatibility
Microencapsulation
Nanoparticles
Nasal delivery
Protein delivery
Pulmonary delivery

ABSTRACT

Chitosan/carrageenan/tripolyphosphate nanoparticles were previously presented as holding potential for an application in transmucosal delivery of macromolecules, with tripolyphosphate demonstrating to contribute for both size reduction and stabilisation of the nanoparticles. This work was aimed at evaluating the capacity of the nanoparticles as protein carriers for pulmonary and nasal transmucosal delivery, further assessing their biocompatibility pattern regarding that application. Nanoparticles demonstrated stability in presence of lysozyme, while freeze-drying was shown to preserve their characteristics when glucose or sucrose were used as cryoprotectants. Bovine serum albumin was associated to the nanoparticles, which were successfully microencapsulated by spray-drying to meet the aerodynamic requirements inherent to pulmonary delivery. Finally, a satisfactory biocompatibility profile was demonstrated upon exposure of two respiratory cell lines (Calu-3 and A549 cells) to the carriers. A negligible effect on cell viability along with no alterations on transepithelial electrical resistance and no induction of inflammatory response were observed.

1. Introduction

Several physicochemical and biopharmaceutical issues make systemic administration of biomolecules a challenging task (Gupta & Sharma, 2009), compelling the need to develop adequate drug delivery systems that overcome inherent limitations. These carriers are mainly developed to avoid the need of parenteral administration, instead permitting effective transmucosal delivery. The pulmonary and nasal routes are increasingly addressed in this context, because of the large absorptive surface and the easy access, respectively, among other characteristics. Carriers are thus designed to exhibit characteristics that improve the epithelial contact, while protecting sensitive bioactive materials from *in vivo* degradation. Nanoparticles are first-line candidates for this end, successfully associating therapeutic macromolecules (Reis, Neufeld, Ribeiro, & Veiga, 2006). A previous study demonstrated the ability of two natural polymers, chitosan (CS) and κ-carrageenan (CRG), to assemble into nanoparticles of 400–600 nm by simple polyelectrolyte complexation (Grenha et al., 2010). While CS is a very well-known material, the abilities of CRG are not sufficiently explored. Apart from the advantage of using natural materials, which facilitates biocompatibility (Malafaya, Silva, & Reis, 2007), the polyelectrolyte complexation between CS and CRG uses very mild conditions, occurring in hydrophilic medium (Grenha, 2012). Nevertheless, the intimate contact between the carrier and the epithelial surface that highly favours mucosal delivery of drugs is reported to be maximal for particles of 50–500 nm (Desai, Labhasetwar, Amidon, & Levy, 1996; Jani, Halbert, Langridge, & Florence, 1990) and strong positive surface charge (Bogataj et al., 2003; Carvalho, Bruschi, Evangelista, & Gremião, 2010). Therefore,

* Corresponding author at: Centre for Molecular and Structural Biomedicine (CBME), Faculty of Sciences and Technology, Building 8, Room 3.1, Campus de Gambelas, 8005-139 Faro, Portugal. Tel.: +351 289800100x7441; fax: +351 289 818419.
E-mail addresses: susananasus@gmail.com (S. Rodrigues), ccordei@ualg.pt (C. Cordeiro), mbegona.seijo@usc.es (B. Seijo), mdelcarmen.remunan@usc.es (C. Remuñán-López), amgrenha@ualg.pt (A. Grenha).

http://dx.doi.org/10.1016/j.carbpol.2015.01.048
0144-8617/

more recently we associated tripolyphosphate (TPP) to the CS/CRG nanoparticle formulation as a cross-linking agent, providing a size decrease and obtaining more stable nanoparticles (Rodrigues, Rosa da Costa, & Grenha, 2012).

Notwithstanding the relevance that nanoparticles have gained in the last decade, the fact is that several limitations are still to overcome regarding their application. The inherent tendency for particle aggregation, chemical instability of polymers and early release of active substances are major problems to be addressed. In addition, as nanoparticles are usually formulated as suspensions, they are prone to microbial growth (Wu, Zhang, & Watanabe, 2011). Therefore, under all aspects, the physical and chemical stability of the systems is expected to be improved if water is removed (Abdelwahed, Degobert, Stainmesse, & Fessi, 2006). The shelf-life of nanoparticles is a relevant aspect of their potential application as drug delivery carriers, especially concerning the need to maintain unaltered physicochemical characteristics along time. Freeze-drying appears in this context as a very adequate choice, ensuring a soft drying procedure. The more aggressive conditions associated to freeze-drying can be softened by the use of specific protectants. These will provide the formation of a solid amorphous glass film around the nanoparticles and the immobilisation of the carriers, preventing aggregation and promoting stabilisation (Beirowski, Inghelbrecht, Arien, & Gieseler, 2011, 2012).

Safety issues are another permanent subject adjacent to nanoparticle applications. In fact, regarding the inhalation of nanoparticles, their fate after administration remains uncertain and there is the possibility of accumulation in the lung tissue upon repeated administrations (Rogueda & Traini, 2007). With regard to the evaluation of materials safety, there is a general recommendation considering that an initial *in vitro* evaluation should comprise different cell lines and times of exposure, while not only cell viability but also the inflammatory response should be determined (ISO, 2009; Rodrigues, Dionísio, Remuñán-López, & Grenha, 2012). The Calu-3 and A549 respiratory epithelial cell lines have been frequently used in this context to evaluate the behaviour of systems aimed at respiratory drug delivery, either nasal or pulmonary (Foster, Avery, Yazdanian, & Audus, 2000; Grenha et al., 2007; Nahar et al., 2013).

In this work, we aimed at exploring the potential of CS/CRG/TPP nanoparticles for an application in nasal and pulmonary transmucosal delivery of proteins, placing a particular emphasis on their biocompatibility behaviour. Additionally, the stability of nanoparticles in presence of lysozyme (an enzyme present in the nasal and lung mucosa), as well as the ability of freeze-drying to provide a dry form of nanoparticle suspensions, were also assessed. Regarding pulmonary administration, as nanoparticles are known to lack the adequate aerodynamic diameter to permit deep lung delivery with success, which should vary between 1 and 5 μm, the strategy of microencapsulating the nanocarriers was applied, following a previously described approach (Grenha, Seijo, & Remuñán-López, 2005).

2. Materials and methods

2.1. Materials

Chitosan (low molecular weight, deacetylation degree = 75–85%), pentasodium tripolyphosphate, bovine serum albumin (BSA), phosphate buffer saline (PBS) tablets pH 7.4, Dulbecco's modified Eagle's medium (DMEM), penicillin/streptomycin (10,000 units/mL, 10,000 μg/mL), non-essential amino acids, L-glutamine 200 mM, trypsin–EDTA solution (2.5 g/L trypsin, 0.5 g/L EDTA), trypan blue solution (0.4%), thiazolyl blue tetrazolium bromide (MTT), sodium dodecyl sulphate (SDS), *N*, *N*-dimethylformamyde (DMF), glycerol, lipopolysacharide (LPS), dimethyl sulfoxide (DMSO), lysozyme and glacial acetic acid were supplied by Sigma Chemicals (Germany). *k*-Carrageenan was obtained from FMC Biopolymer (Norway) and foetal bovine serum (FBS) was from Gibco (USA). Ultrapure water (Milli-Q Plus, Millipore Iberica, Spain) was used throughout.

2.2. Cell lines

The Calu-3 and A549 cell lines were obtained from the American Type Culture Collection (Rockville, USA) and used between passages 35–45 and 20–30, respectively. Cell cultures were grown in 75 cm^2 flasks in a humidified 5% CO_2/95% atmospheric air incubator at 37 °C. For both cell lines, cell culture medium (CCM) was DMEM supplemented with 10% (v/v) FBS, 1% (v/v) non-essential amino acids solution, 1% (v/v) L-glutamine solution (200 mM) and 1% (v/v) penicillin/streptomycin. Medium was exchanged every 2–3 days and cells were subcultured weekly in the case of A549 cells and every 10–15 days for Calu-3 cell line.

2.3. Preparation of CS/CRG/TPP nanoparticles

CS/CRG/TPP nanoparticles were prepared as described previously (Rodrigues, Rosa da Costa, et al., 2012) based on the polyelectrolyte complexation of CS with CRG and additional ionic gelation of chitosan with TPP anions. After an initial optimisation, a final theoretical CS/CRG/TPP ratio of 4/1/1 (w/w) was selected to perform the studies (4/1/0 for control nanoparticles). Briefly, CS was dissolved in 1% (w/w) acetic acid to obtain a solution of 1 mg/mL. CRG and TPP were dissolved in purified water and mixed to obtain a solution where the concentration of each polymer is 0.63 mg/mL. The spontaneous formation of nanoparticles occurs upon incorporation of 0.8 mL of a solution of CRG/TPP or CRG into 2 mL of the CS solution, under gentle magnetic stirring at room temperature.

The association of BSA to the nanoparticles was performed by dissolving the protein in water and mixing with a previously prepared mixture of CRG/TPP solution, prior to the addition to CS solution, as described above. The amount of BSA associated to each batch was calculated to represent a theoretical content of 30% (w/w) of the amount of CS.

Nanoparticles were concentrated by centrifugation at 16,000 × *g* on a 10 μL glycerol layer for 30 min at 15 °C (Heraeus Fresco 17 centrifuge, Thermo scientific, USA). After discarding the supernatants, the nanoparticles were resuspended in 200 μl of purified water.

When no further indication is provided, 'CS/CRG/TPP nanoparticles' refer to mass ratios 4/1/1.

2.4. Characterisation of nanoparticles

2.4.1. Determination of production yield

The nanoparticle production yield was calculated by gravimetry. Fixed volumes of nanoparticle suspensions were centrifuged (16,000 × *g*, 30 min, 15 °C), and sediments were freeze-dried over 24 h at −34 °C, followed by a gradual increase in temperature until 20 °C, using a Labconco freeze dryer (Labconco, USA) ($n = 3$). The yield of nanoparticle production (PY) was calculated as follows:

$$PY = \frac{\text{Nanoparticle sediment weight}}{\text{Total solids weight}} \times 100 \quad (1)$$

where nanoparticle sediment weight is the weight after freeze-drying and total solids weight is the total amount of solids added for nanoparticle formation.

2.4.2. Morphological observation

The morphological examination of CS/CRG/TPP nanoparticles was conducted by transmission electron microscopy (TEM)

(JEM-1011, JEOL, Japan). The samples were stained with 2% (w/v) phosphotungstic acid (Carvalho, Grenha, Remunan-Lopez, Alonso, & Seijo, 2009) and placed on copper grids with carbon films (Ted Pella, USA) for TEM observation.

2.4.3. Physicochemical properties

Measurements of nanoparticle size and zeta potential were performed on freshly prepared samples by photon correlation spectroscopy and laser Doppler anemometry, respectively, using a Zetasizer Nano ZS (Malvern Instruments, Malvern, UK). For the analysis of particle size and determination of the electrophoretic mobility, each sample was diluted to the appropriate concentration with ultrapure water and placed in the electrophoretic cell. Each analysis was performed at 25 °C. Three batches of each formulation were analysed ($n = 3$).

2.4.4. Determination of BSA association capacity

The amount of non-encapsulated BSA was determined in the supernatant by reverse phase-high performance liquid chromatography (RP-HPLC; Agilent 1100 series, Germany). The chromatographic conditions were adapted from Umrethia, Kett, Andrews, Malcolm, and Woolfson (2010) as follows: Aeris widepore 3.6u XB-C18 300A column 4.6 mm i.d. × 250 mm length with security guard cartridge (Phenomenex, UK); run temperature 25 °C; gradient flow (0.1% TFA in water (A), 0.1% TFA in acetonitrile (B); A/B from 95:5 to 35:65 in 10 min) mobile phase, total run time 15 min, UV detection at 280 nm; flow rate 1.0 mL/min; injection volume 20 μL; BSA retention time 8.8 min. A linear calibration plot for BSA in the different solvents (acetic acid solution, PBS pH 7.4 and buffer pH 6.8) was obtained over the range 10–120 μg/mL ($n = 3$). BSA association efficiency (AE) and nanoparticle loading capacity (LC) were calculated as follows:

$$\text{AE} = \frac{(\text{Total amount of BSA} - \text{free amount of BSA})}{\text{Total amount of BSA}} \times 100 \quad (2)$$

$$\text{LC} = \frac{(\text{Total amount of BSA} - \text{free amount of BSA})}{\text{Nanoparticle weight}} \times 100 \quad (3)$$

2.5. Evaluation of nanoparticle stability in the presence of lysozyme

The stability of CS/CRG/TPP nanoparticles (4/1/0 and 4/1/1) was analysed in presence of lysozyme. To do so, nanoparticle suspensions at a concentration of 1 mg/mL were incubated with lysozyme (0.2 and 0.8 mg/mL) (Grenha et al., 2005) at 37 °C under mild horizontal shaking, for 120 min. At appropriate time intervals (30, 60, 90 and 120 min), the size and zeta potential of nanoparticles were measured, as described above ($n = 3$).

2.6. Nanoparticle stability upon freeze-drying

With the aim of developing a pharmaceutically acceptable dry form of the nanoparticle suspensions, CS/CRG/TPP nanoparticles were submitted to a freeze-drying study. Different concentrations of nanoparticles (1, 2 and 4 mg/mL) and different cryoprotectants (trehalose, lactose, sucrose and glucose) at varied concentrations were tested as variables in the optimisation of nanoparticle stabilisation by freeze-drying. To perform the study, 1 mL of unloaded nanoparticles was freeze-dried in the presence of 5 or 10% (w/v) of cryoprotectant. The freeze-drying process occurred at a pressure of 50–100 Torr and consisted of 24 h of primary drying, starting at −35 °C and gradually increasing to −10 °C, 24 h at 0 °C and a final step of secondary drying (12–24 h) at 15 °C (Labconco Corp., USA). After freeze-drying, nanoparticle suspensions were reconstituted by adding the volume of water corresponding to the initial volume (1 mL), and their size and zeta potential were determined as indicated above ($n = 3$).

The conditions found to better maintain the original properties of unloaded nanoparticles were applied on BSA-loaded nanoparticles. In this case, nanoparticle concentrations of 1 and 2 mg/mL were freeze-dried with both glucose and sucrose at a concentration of 10% (w/w).

2.7. Preparation of microencapsulated nanoparticles

Mannitol was selected as matrix material for the production of microparticles, as was previously described (Grenha et al., 2005). An aqueous solution of the excipient was prepared at a concentration of 1.6% (w/v). Upon centrifugation, CS/CRG/TPP nanoparticles were resuspended with the mannitol solution instead of water, in order to obtain a mannitol/nanoparticle ratio of 80/20 (w/w). The final solid concentration of the suspensions was 2% (w/v).

Dry powders were obtained by spray-drying the previously prepared suspension using a laboratory-scale spray-dryer (Buchi® Mini Spray Dryer, B-290, Buchi, Switzerland).

The spray-drying conditions were: feed rate of 2.5 mL/min, two fluids external nozzle 0.7 mm, inlet temperature of 160 ± 2 °C, outlet temperature of 95 ± 3 °C. The airflow rate and the aspirator were kept constant at 400 Nl/h and 80%, respectively. The spray-dried powders were collected and stored in a desiccator at room temperature until use.

2.8. Characterisation of microencapsulated nanoparticles

2.8.1. Determination of spray-drying yield

The spray-drying yield was calculated by gravimetry, comparing the total amount of solids initially added for the preparation of microencapsulated nanoparticles (CS + CRG + TPP + BSA + mannitol) with the amount of resulting microspheres ($n = 3$). The following equation was used for the calculation:

$$\text{Yield (\%)} = \frac{\text{Microspheres weight}}{\text{Total solids weight}} \times 100 \quad (4)$$

2.8.2. Morphological and aerodynamic characterisation

The morphological characterisation of microspheres was performed using a field emission scanning electron microscope (FESEM; FESEM Ultra Plus, Zeiss, Germany) at 3 kV of voltage, which is equipped with a secondary electron (SE) detector. The dry powders were placed onto metal plates and a 5 nm thick gold palladium film was sputter-coated on the samples (Q150T S/E/ES Sputter Coater, Quorum Technologies, UK) before viewing.

The particle size was estimated as the Feret's diameter (distance between two tangents on opposite sides of the particles) and was directly determined with an optical microscope (Olympus IX51, Japan). The estimation was based on the mean diameter resulting from the evaluation of 300 particles ($n = 300$).

Real density was determined using a Helium Pycnometer (Micropycnometer, Quanta Chrome, model MPY-2, USA) ($n = 3$). Apparent tap density was obtained by measuring the volume of a known weight of powder in a 10 mL test-tube after mechanical tapping (30 tap/min, Tecnociencia, Spain). After registration of the initial volume, the test-tube was submitted to tapping until constant volume was achieved, according to a previously described method (El-Gibaly, 2002) ($n = 3$).

The aerodynamic diameter was obtained using a TSI Aerosizer® LD equipped with an Aerodisperser® (Amherst Process Instrument Inc., Amherst, MA, USA) and assuming real density as the density parameter for the determination of the aerodynamic diameter.

2.9. In vitro biocompatibility study

2.9.1. Evaluation of metabolic activity

The *in vitro* cytotoxicity of CS/CRG/TPP nanoparticles, microencapsulated nanoparticles (mannitol/nanoparticles = 80/20, w/w), as well as that of the raw materials involved in nanoparticle production, was assessed by the metabolic assay thiazolyl blue tetrazolium bromide (MTT) test. Two cell lines representative of pulmonary and nasal epithelia (Calu-3 and A549 cells) were used. A549 cells were seeded at a density of 1×10^4 cells/well and Calu-3 cells at 2×10^4 cells/well in 96-well plates, in 100 μl of the same medium used for culture in cell culture flasks. The cells were grown at 37 °C in a 5% CO_2 atmosphere for 24 h before use (Grenha et al., 2007).

Three different concentrations (0.1, 0.5 and 1.0 mg/mL) of nanoparticles were evaluated for cytotoxicity over 3 and 24 h. Suspensions of unloaded nanoparticles and microencapsulated nanoparticles, BSA loaded nanoparticles and solutions of the individual raw materials (CS, CRG and TPP) were evaluated separately for cytotoxicity. Sodium dodecyl sulphate (SDS, 2%, w/v) was used as a positive control of cell death. Optimal cell seeding density and the absence of MTT conversion in the assay medium were confirmed in preliminary experiments. All formulations and controls were prepared as solution/suspensions in pre-warmed CCM without FBS immediately before application to the cells.

To initiate the assay, culture medium of cells at 24 h in culture was replaced by 100 μL of fresh medium without FBS containing the test samples or controls. After 3 or 24 h of cell incubation, samples/controls were removed and 30 μL of the MTT solution (0.5 mg/mL in PBS, pH 7.4) were added to each well. After 2 h, any generated formazan crystals were solubilised with 50 μL of DMSO. Upon complete solubilisation of the crystals, the absorbance of each well was measured by spectrophotometry (Infinite M200, Tecan, Austria) at 540 nm and corrected for background absorbance using a wavelength of 650 nm (Carmichael, DeGraff, Gazdar, Minna, & Mitchell, 1987).

The relative cell viability (%) was calculated as follows:

$$\text{Viability}\,(\%) = \frac{(A - S)}{(\text{CM} - S)} \times 100 \quad (5)$$

where A is the absorbance obtained for each of the concentrations of the test substance, S is the absorbance obtained for the 2% SDS and CM is the absorbance obtained for untreated cells (incubated with CCM). The latter reading was assumed to correspond to 100% cell viability. The assay was performed on three occasions with six replicates at each concentration of test substance in each instance.

2.9.2. Determination of inflammatory response

The inflammatory response generated by the exposure to nanoparticles and microencapsulated nanoparticles was evaluated on Calu-3 cells. To perform the assay, the cells were seeded on 96-well plates (2×10^4 cells/well) and, after 24 h incubation at 37 °C in 5% CO_2 atmosphere, exposed to nanoparticles and microencapsulated nanoparticles at a concentration of 1 mg/mL. The exposure to lipopolysaccharide (LPS; 10 μg/mL) was used as positive control (Alfaro-Moreno et al., 2009; Mura et al., 2011), while cells incubated with CCM were used as negative control. All formulations and controls were prepared as solutions/suspensions in pre-warmed CCM without FBS immediately before application to the cells. After 24 h of exposure, the cell supernatants were collected and centrifuged (10 min, 16,000 × *g*, 15 °C, centrifuge 5804R, Eppendorf, Germany). The levels of IL-6 and IL-8 existing in Calu-3 cell supernatants were determined by quantitative ELISA using human IL-6 and IL-8 Quantikine ELISA kits (R&D Systems, Minneapolis, MN), according to the manufacturer's instructions. The supernatants were appropriately diluted (approximately 10 times for IL-6 and 50 times for IL-8). The assay was performed on three occasions with two replicates of test substance in each instance. The concentration of individual cytokines for each sample is expressed as percentage of the control (incubation with CCM) from triplicate assays.

2.9.3. Evaluation of epithelial integrity

For the studies of epithelial integrity, Calu-3 cells were cultured at an air interface according to a previously described methodology (Grainger, Greenwell, Lockley, Martin, & Forbes, 2006). Briefly, 100 μL of Calu-3 cell suspension was seeded at a density of 5×10^5 cells/cm^2 in Transwell inserts (0.33 cm^2), with 0.5 mL medium in the basolateral chamber. The cells were incubated at 37 °C, 5% CO_2 for 2 days. After this time, the medium was aspirated from the apical and basolateral chambers and replaced only in the basolateral chamber, the apical chamber being exposed to the incubator atmosphere. Medium was replaced every 2 days thereafter.

In order to verify the effect of nanoparticles on Calu-3 cell layer integrity, the formulations were dispersed in 100 μL FBS-free CCM at a concentration of 1 mg/mL and incubated with the cell layers. Transepithelial electrical resistance (TER) was measured using chopstick electrodes and an EVOM® volt metre (STX-2 and Evom G, World Precision Instruments, UK). TER measurements were taken 30 min before the experiment and at 0.5, 1, 2, 4, 6, 24 and 48 h after administration. TER values were calculated by subtracting the resistance of cell-free culture inserts and correcting for the surface area of the Transwell insert. Cell layers incubated with CCM were used as the reference (control), from which TER changes during exposure to the samples were calculated. All experiments were performed in triplicate on three occasions.

2.10. Statistical analysis

For the generality of results, the *t*-test and the one-way analysis of variance (ANOVA) with the pairwise multiple comparison procedures (Dunn's method) were performed to compare two or multiple groups, respectively.

The freeze-drying case study determines the effect of different cryoprotectants and nanoparticle concentration on nanoparticle stability. Due to the number of observations involved (three to four) in each cell/treatment and to the existence of empty cells, a more complex statistical methodology was not applied, because it would compromise the model assumptions and result in misleading inferences. Therefore, the statistical approach used for this analysis was the one-way ANOVA with Gowes-Howell *post hoc* tests, based on sample sizes and variance homogeneity between groups.

The factorial design (FD) is often used for manipulative experiments, such as that of the metabolic activity (MTT test). In that case, for both cell lines tested (Calu-3 and A549) the effect of sample type (X_1) and concentration (X_2) on cell viability (Y). Each of the factors (X_1 and X_2) has three levels. In the case of X_2 the levels are 0.1, 0.5 and 1.0 mg/mL. For X_1 there is a split in two groups: (1) when raw materials are considered the levels of X_1 are CS, CRG and TPP; (2) when carrier formulations are studied, the levels are unloaded nanoparticles, BSA-loaded nanoparticles, microencapsulated nanoparticles. For either raw materials or carrier formulations, the objective is to investigate the influence of factors X_1 and X_2 on the response variable (Y). FD was originally planned with equal number of observations per treatment, but some occurrences related to random loss of observations or to practical constraints, cause inequality of sample sizes. Therefore, for the four multifactor designs present in this study, three were unbalanced with observations in every cell/treatment. For this complex FD, the type III sum of squares (SS) was used, because it is not influenced by the sample size in each treatment. The basic multivariate assumptions to be checked are that the errors are independent, normally distributed and have constant variance. Further

analyses with *post hoc* tests Hochberg's GT2 (unbalanced FD) and Tukey, were used to determine which groups differ.

The statistical analyses were performed with the software SPSS (version 22.0 for windows) considering a significance level of $\alpha = 0.05$.

3. Results and discussion

CS/CRG/TPP nanoparticles were previously reported by our group in a work that evidenced the ability of TPP to decrease nanoparticle size and improve stability (Rodrigues, Rosa da Costa, et al., 2012). In that work, the potential of the carriers for transmucosal drug delivery was suggested. More recently we have observed the ability of these nanocarriers to associate different proteins, demonstrating that the pH of the nanoparticle assembly medium has a strong effect on protein association and the pH of the release medium affects the release profile (unpublished results). The present work is dedicated to the study of these nanoparticles regarding an application in nasal and pulmonary delivery.

3.1. Characterisation of CS/CRG/TPP nanoparticles

After an initial screening of varied CS/CRG/TPP mass ratios, seeking for the formulation that produces nanoparticles with the most suitable characteristics for the objective of transmucosal delivery (Rodrigues, Rosa da Costa, et al., 2012), the formulation CS/CRG/TPP = 4/1/1 (w/w) was selected for subsequent studies. The corresponding formulation without TPP (CS/CRG/TPP = 4/1/0, w/w) was used as control in some of the performed studies to show the effect of the inclusion of TPP.

Fig. 1A depicts the result of the morphological evaluation of BSA-loaded nanoparticles, which evidence a spherical structure similar to both unloaded nanoparticles (Rodrigues, Rosa da Costa, et al., 2012) and to polysaccharide-based nanoparticles in general (Goycoolea, Lollo, Remunan-Lopez, Quaglia, & Alonso, 2009; Oyarzun-Ampuero, Brea, Loza, Torres, & Alonso, 2009; Zorzi, Párraga, Seijo, & Sánchez, 2011).

As shown in Table 1, the developed BSA-loaded nanoparticles evidence adequate physicochemical properties for the objective of transmucosal delivery, with a size around 300 nm and a positive zeta potential (+40 mV). In fact, the size is small enough to permit an intimate contact with epithelial surfaces, which is maximal at 50–500 nm (Desai et al., 1996; Jani et al., 1990). In turn, the high positive zeta potential further potentiates the interaction with epithelia, as this is negatively charged and, thus, an electrostatic interaction is enabled. In summary, these characteristics are expected to provide a prolonged retention of nanoparticles close to epithelial surfaces, potentiating protein release. Notwithstanding the importance of these physicochemical features, the presence of mucus and the mechanism of mucociliary clearance also need to be considered regarding the success of nasal and pulmonary transmucosal delivery (Dombu & Betbeder, 2013; Marttin, Schipper, Verhoef, & Merkus, 1998). Nanoparticles described in this work are expected to exhibit bioadhesive properties to some extent, due to the chitosan content. Besides the proper chitosan ability to adhere to biological substrates (Du, Cai, & Zhai, 2014; Lehr, Bouwstra, Schacht, & Junginger, 1992), chitosan-based nanoparticles have also demonstrated the same capacity in several occasions (Bernkop-Schnürch, Weithaler, Albrecht, & Greimel, 2006; Sandri et al., 2010). This will possibly improve the carrier residence time close to the epithelia, potentiating drug absorption (Dombu & Betbeder, 2013; Marttin et al., 1998). Additionally, nanoparticles have been reported to avoid or delay mucociliary clearance, although this ability is highly dependent on their size and is more relevant for particles below 100 nm (Oberdörster, Oberdörster, & Oberdörster, 2005; Sung, Pulliam, & Edwards, 2007).

It is also observed in the table that the inclusion of TPP in the formulation increases the nanoparticle production yield, while maintaining the encapsulation efficiency, which is around 50%. A great difference is observed in loading capacity, which is of 70% for CS/CRG/TPP = 4/1/0 and approximately 30% for 4/1/1. This difference is explained by the fact that, while both formulations encapsulate a similar amount of protein, the nanoparticles containing TPP display a considerably higher production yield. Therefore, as viewed in Eq. (3), there is the same amount of protein distributed by a higher amount of total solids, thereby resulting in a lower value of loading capacity. Unloaded nanoparticles display somewhat different physicochemical characteristics, 4/1/0 nanoparticles having 491 nm and +78 mV and 4/1/1 nanoparticles displaying a size of 208 nm and +47 mV (data not shown).

3.2. Evaluation of nanoparticle stability in presence of lysozyme

Lysozyme is an enzyme that is present in mucosal surfaces, including the nasal and pulmonary (Konstan et al., 1981; Muzzarelli, 1997), which exhibits the ability to cleave β-(1–4) glycosidic bonds of chitosan (Muzzarelli, 1997). Therefore, taking into account the high content of chitosan present in the proposed nanoparticles, evaluating their behaviour in presence of this enzyme is important regarding a future interpretation of results, such as those obtained *in vivo*. To perform the evaluation, nanoparticles were incubated with lysozyme (0.2 and 0.8 mg/mL) at 37 °C and their size and zeta potential were monitored along time. The enzyme concentration of 0.2 mg/mL was used taking into account indications found in the literature regarding physiological concentrations of the enzyme (Konstan et al., 1981). Furthermore, a concentration of 0.8 mg/mL was chosen to investigate the nanoparticle behaviour in extreme conditions, as previously reported (Grenha et al., 2005).

As observed in Fig. 2, the formulation of nanoparticles without TPP (CS/CRG) showed a tendency for size decrease along time. When lysozyme was present at a concentration of 0.2 mg/mL, the decrease was not significant, as high standard deviations are obtained. However, at 0.8 mg/mL a strong and significant size decrease ($p < 0.05$) occurs up to 60 min of incubation, although after that a sudden increase in size is observed, inverting the trend. This is probably due to aggregation, as a concomitant increase in the standard deviation of the mean size is observed, indicating a great dispersion of sizes. Zeta potential, in turn, remained stable during the assay (data not shown). Interestingly, the formulation containing TPP was not affected by the presence of the enzyme, no significant size reduction being observed independently of the concentration of lysozyme. This behaviour reveals a somewhat protecting effect attributed by TPP.

An absence of effect of the enzyme on chitosan-based nanoparticles (also containing TPP) incubated in similar conditions was previously reported in another study (Vila, Sánchez, Tobío, Calvo, & Alonso, 2002). It is possible that the inclusion of TPP, which acts as cross-linker, prevents or at least modifies chitosan exposure, thus not enabling an easy and rapid enzymatic degradation as is seen for nanoparticles devoid of TPP.

3.3. Evaluation of nanoparticle stability upon freeze-drying

When nanocarriers are formulated as aqueous suspensions, both physical (aggregation/particle fusion) and chemical (hydrolysis of polymer and chemical reactivity) instability phenomena are known to appear at some point (Abdelwahed et al., 2006; Chacón, Molpeceres, Berges, Guzmán, & Aberturas, 1999; Kumar, Shafiq, & Malhotra, 2012), limiting nanoparticle applications (Sameti

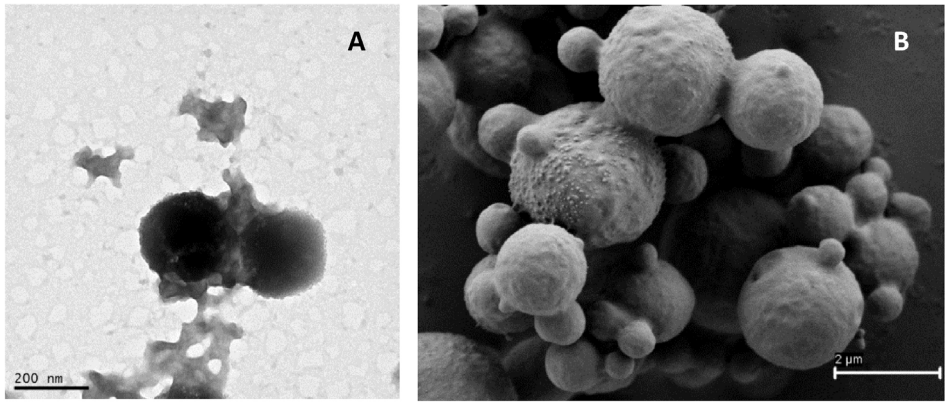

Fig. 1. (A) TEM microphotograph of BSA-loaded CS/CRG/TPP (4/1/1, w/w) nanoparticles; (B) SEM microphotograph of microspheres composed of mannitol/nanoparticles = 80/20 (w/w).

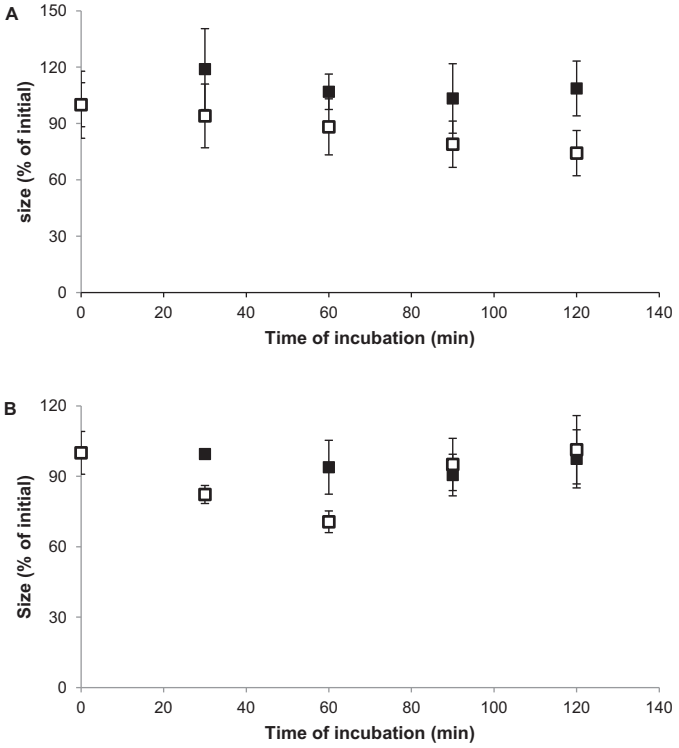

Fig. 2. Size evolution as a function of time upon incubation of CS/CRG/TPP nanoparticles (□) mass ratio 4/1/0 and (■) mass ratio 4/1/1, with (A) 0.2 mg/mL and (B) 0.8 mg/mL lysozyme, at 37 °C (mean ± SD, $n = 3$).

et al., 2003; Wu et al., 2011). Aqueous suspensions of CS/CRG/TPP nanoparticles were reported in a previous work to remain stable for up to 9 months, the presence of TPP in the formulation demonstrating to have a significant role in this effect (Rodrigues, Rosa da Costa, et al., 2012). However, the preference in storing and transporting products in dry state, has led to the decision of developing a lyophilised formulation. Regarding the present work, it is important to recall that a nasal formulation of nanoparticles will involve a suspension, while microencapsulated nanoparticles (dry powders) are proposed for lung delivery. Still, in the latter case there might be a time period between nanoparticle production and microencapsulation where a lyophilised form of nanoparticles will be beneficial for storage.

Freeze-drying has been considered an adequate technique to improve the long-term stability of colloidal nanoparticles. Nevertheless, it is a complex process that requires a major optimisation of the inherent conditions. Many parameters of the formulation/process may decide the success of freeze-drying (Abdelwahed et al., 2006). In this study, nanoparticles were freeze-dried using different sugars as cryoprotectants, at varied concentrations. The concentration of nanoparticle suspensions was also tested as variable. The direct freeze-drying of nanoparticles (without cryoprotectants) did not permit the preservation of their properties (data not shown), leading to strong aggregation. This effect might be explained by both the high concentration of particles undergoing the freezing step and the mechanical stress induced by ice crystallisation (Abdelwahed et al., 2006; Vauthier & Bouchemal, 2009). This observation was reported in a previous work of our group for nanoparticles composed of other polysaccharides (Dionísio et al., 2013), as well as in other works available on the literature (Abdelwahed et al., 2006; Fuente, Seijo, & Alonso, 2008).

The purpose of this study was thus examining the effects of type of cryoprotectant (sucrose, trehalose, lactose and glucose), cryoprotectant concentration (5% and 10%, w/w) and nanoparticle concentration (1, 2 and 4 mg/mL) on the nanoparticle characteristics upon reconstitution with water from the corresponding lyophilised powder.

Fig. 3 displays the variation of nanoparticle size when comparing the obtained value after reconstitution of freeze-dried material (Df) with that initially determined (Di) before the freeze-drying process. As a first approach, unloaded nanoparticles were used. The ANOVA experiment revealed that the concentration of nanoparticle suspensions to be freeze-dried is the sole parameter evidencing a relevant and statistically significant effect on the stability conferred by the cryoprotectants. In this regard, the *post hoc* test (Gowes-Howell) shows that using nanoparticle concentrations of 2 mg/mL or 4 mg/mL leads to a higher increase of nanoparticle size ($p < 0.05$)

Table 1
Physicochemical properties, production yield and encapsulation data of BSA-loaded CS/CRG/TPP (4/1/1, w/w) nanoparticles (mean ± SD, $n = 3$).

CS/CRG/TPP formulation	Size (nm)	ζ Potential (mV)	Production yield (%)	Encapsulation efficiency (%)	Loading capacity (%)
4/1/0 loaded	226 ± 35	+27 ± 5	15 ± 2	51 ± 12	70 ± 18
4/1/1 loaded	327 ± 32	+40 ± 5	30 ± 2	48 ± 8	27 ± 5

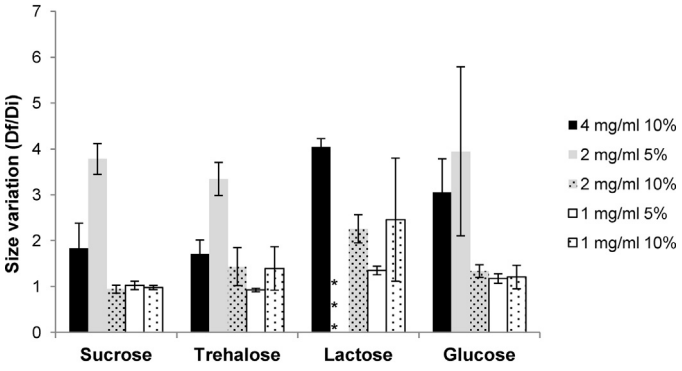

Fig. 3. Size variation of CS/CRG/TPP nanoparticles upon freeze-drying at different concentrations, in presence of 5% or 10% sucrose, trehalose, lactose and glucose, and further reconstitution in water (hydrodynamic diameter of nanoparticles before (Di) and after (Df) freeze-drying). Results represent mean ± SD ($n = 3$); *** indicates formation of precipitate.

as compared with 1 mg/mL, which is the concentration permitting the desired maintenance of size after freeze-drying.

Zeta potential values did not evidence alterations after freeze-drying in any of the tested conditions (data not shown). Other works studying the freeze-drying of comparable concentrations of polysaccharide-based nanoparticles have reported good stabilisation provided by the same or similar cryoprotectants (de la Fuente et al., 2008; Dionísio et al., 2013; Hirsjärvi, Peltonen, & Hirvonen, 2009).

Although not to a statistically significant manner, other interpretations might be suggested by Fig. 3. Regarding the performance of the distinct cryoprotectants that were tested, it is important to observe that lactose (a typical excipient used in lung delivery) revealed absolutely inefficient as cryoprotectant agent, not preventing particle aggregation after freeze-drying. This poor protective effect was also observed in a previous work of the group with other polysaccharide-based nanoparticles (Dionísio et al., 2013) and was further reported in the literature, being attributed to an ineffective protection during the freezing step (Hirsjärvi et al., 2009). Sucrose, glucose and trehalose (in this order) are suggested to have better ability as cryoprotectants, as their presence provided a more adequate maintenance of the initial characteristics of nanoparticles, at least under certain conditions. Sucrose maintained the exact characteristics of nanoparticles when used at 10% (with the already mentioned exception of the 4 mg/mL concentration of nanoparticles) or at 5% when nanoparticles are freeze-dried at the lower concentration tested. A very satisfactory cryoprotective effect provided by both glucose and sucrose was previously reported by our group regarding the stabilisation of two formulations of pullulan-based nanoparticles (sulfated pullulan/chitosan and carrageenan/aminated pullulan) (Dionísio et al., 2013). The concentration of the cryoprotectant is also an important parameter to optimise. In this regard, a content of 5% was generally found to be enough to stabilise nanoparticles freeze-dried at a concentration of 1 mg/mL, while an increase to 10% of cryoprotectant is needed when the nanoparticle concentration increases to 2 mg/mL.

Considering the results obtained with unloaded nanoparticles, BSA-loaded nanoparticles at the concentration of 1 and 2 mg/mL were freeze-dried with 10% of both glucose and sucrose. The physicochemical characteristics of the nanoparticles were still maintained (data not shown). However, it was previously referred that the use of glucose as cryoprotectant of protein formulations should be cautious because of its reducing character (Li et al., 1996; Wang, 2000). Nevertheless, the freeze-drying of protein nanocarriers in presence of glucose has been reported as efficient, considering both the physicochemical stability of the carrier and the maintenance of protein properties (Freixeiro et al., 2013). In any case, a comprehensive review on the subject suggests that any evaluation should be performed on a case-by-case basis (Wang, 2000).

This study evidences the suitability of using freeze-drying to obtain nanoparticles in a dry form, but it reinforces the importance of carefully selecting and optimising the conditions of the freeze-drying process in order to achieve an optimised protective effect.

3.4. Microencapsulation of nanoparticles

The success of inhalable formulations is primarily dependent on their aerodynamic properties, as these influence both the dispersion and sedimentation pattern of the carriers (Sung et al., 2007). When a systemic action is intended, the drug carriers should be small enough to pass through the mouth, throat and conducting airways and reach the deep lung, but not so small that they fail to deposit and are breathed out again. In this context, it has been considered that an aerodynamic diameter between 1 and 5 μm is necessary (Bosquillon, Lombry, Préat, & Vanbever, 2001), which in some cases is even narrowed to 2–3 μm (Oberdörster et al., 2005). A specific conjugation between size and density of the carriers is, thus, necessary. The pulmonary administration of nanoparticles is severely hindered by their low inertia, which makes alveolar deposition practically impossible, mainly resulting in the exhalation of the carriers (Sung et al., 2007). The spray-drying of CS-based nanoparticles was first reported by Grenha et al. (2005) as a strategy to endow the nanoparticles with the ability to reach the deep lung. This strategy was later on followed by other groups (Li et al., 2010; Pourshahab et al., 2011). In the present work, the microencapsulation of CS/CRG/TPP nanoparticles was approached to obtain a drug delivery system that permitted efficient administration of the developed nanocarriers aimed at the systemic pulmonary delivery of proteins. Mannitol was selected to compose the matrix of microparticles, as it has demonstrated to simply act as carrier of nanoparticles, providing their release upon reaching the alveoli (Grenha et al., 2005).

Microencapsulated nanoparticles were produced by spray-drying a suspension of mannitol/nanoparticles (80/20, w/w), evidencing a spherical shape and a slightly corrugated surface, as can be observed in Fig. 1B. The nanoparticle carriers were determined to have a Feret diameter of 2.3 ± 0.6 μm, a real density of 1.44 ± 0.01 g/cm^3 and a tap density of 0.42 ± 0.04 g/cm^3. The aerodynamic diameter was determined to be 1.80 ± 0.11 μm. Comparable results were reported for microencapsulated CS/TPP nanoparticles (Grenha et al., 2005), a system that already demonstrated its efficacy *in vivo* for the administration of insulin (Al-Qadi, Grenha, Carrión-Recio, Seijo, & Remuñán-López, 2012). Good indications are thus provided on the capacity of the developed system to act as carrier of nanoparticles to the lung with the aim of a systemic delivery of proteins. Nevertheless, using this approach of microencapsulating the nanoparticles could possibly pose an extra limitation, regarding the high proportion of excipients that need to be used and, consequently, the inherent lower loading. Taking into account that administrations of around 160–180 mg of dry powder have been reported (Hoppentocht, Hagedoorn, Frijlink, & de Boer, 2014; Labiris, Holbrook, Chrystyn, Macleod, & Newhouse, 1999) and considering a protein loading of 27% in nanoparticles and the 20% amount of nanoparticles in the final microparticle formulation, 160 mg would carry approximately 9 mg of protein. This amount is considered suitable for the purpose of obtaining a therapeutic effect and will possible not compromise the success of the formulation, which will obviously be dependent on several other parameters.

3.5. In vitro biocompatibility study

Evaluating the biocompatibility of drug delivery formulations is nowadays a mandatory aspect to address (Gaspar & Duncan, 2009). While an accurate determination of the toxicity of a formulation can only be determined *in vivo*, a variety of *in vitro* toxicological assays, performed in adequately selected cell lines, might provide very useful information and are widely accepted as first indicators (ISO, 2009; Rodrigues, Dionísio, et al., 2012). Current international guidelines require the evaluation to be contextualised with a specific route of administration and dose of the material (Gaspar & Duncan, 2009). It is also referred that polymers and polymer-based carriers should be regarded as different entities and, thus, evaluated separately (Aillon, Xie, El-Gendy, Berkland, & Forrest, 2009; Gaspar & Duncan, 2009; Williams, 2008). This is based on the assumption that the proper carrier structure, among other parameters, might affect the final toxicological behaviour (Aillon et al., 2009; Gaspar & Duncan, 2009).

To address the above mentioned issues, the evaluation of the biocompatibility of CS/CRG/TPP nanoparticles and corresponding raw materials, was performed in this study by means of three different assays, (1) the metabolic activity (MTT), (2) the inflammatory response (detection of IL-6 and IL-8) and (3) the epithelial integrity (measurement of TER). Calu-3 and A549 were the selected cell lines, as they are representative of the respiratory epithelia. Calu-3 is an immortalised cell line obtained from lung adenocarcinoma and has been extensively used in the study of formulations designed for either nasal or pulmonary drug delivery, as it is considered a model of the epithelium of both regions (Casettari et al., 2010; Grainger et al., 2006; Zhu, Chidekel, & Shaffer, 2010). Importantly, Calu-3 cells form tight junctions *in vitro* (Winton et al., 1998) and, under suitable culture conditions, exhibit *in vivo*-like barrier properties (Grainger et al., 2006). A549 is a cell line representative of the alveolar epithelium, obtained from human alveolar adenocarcinoma, showing no ability to form functional tight junctions in culture (Forbes & Ehrhardt, 2005; Foster, Yazdanian, & Audus, 2001; Winton et al., 1998). Consequently, it cannot be used in studies of the epithelial barrier integrity, although this does not prevent their use in cytotoxicity studies.

3.5.1. Evaluation of metabolic activity (MTT assay)

The MTT assay provides an evaluation of the cell metabolic activity upon exposure to the samples and has been used very frequently in the assessment of drug delivery carriers (Rodrigues, Dionísio, et al., 2012). It evaluates the ability of the cells to reduce the MTT reagent to tetrazolium salts, an action that is dependent on mitochondrial metabolism. A reduction of cellular metabolic activity is generally accepted as an early indicator of cellular damage (Scherließ, 2011).

In this work, A549 and Calu-3 cells were cultured and exposed to different concentrations of nanoparticles and raw materials for both a short (3 h) and a more prolonged period (24 h). The exposure for 3 h did not lead to significant decrease in cell viability, with values remaining close to 90–100% in all cases. The only exception occurred for A549 cells exposed to chitosan (data not shown), an effect commented later. In contrast, the prolongation of exposure up to 24 h induces some variability on cell viability. In this manner, for the contact time of 24 h a factorial design was approached to examine the effect of sample type (raw materials/carrier formulations; X_1) and concentration (X_2) on cell viability (Y), for each cell line. The two factors (X_1, X_2) of the experimental design have three levels each, resulting in nine factor/level combinations.

Cell viability results obtained upon 24 h exposure are depicted in Fig. 4 (Calu-3 cells) and 5 (A549 cells). For Calu-3 cells, an unbalanced FD was used in the group of raw materials and formulations. For the raw materials (Fig. 4A), a significant effect ($p < 0.05$) was detected for each of the main factors (X_1 and X_2) and their interaction ($X_1{}^*X_2$). The most relevant observation is that TPP induced a greater decrease of cell viability as compared to CS and CRG ($p < 0.05$).

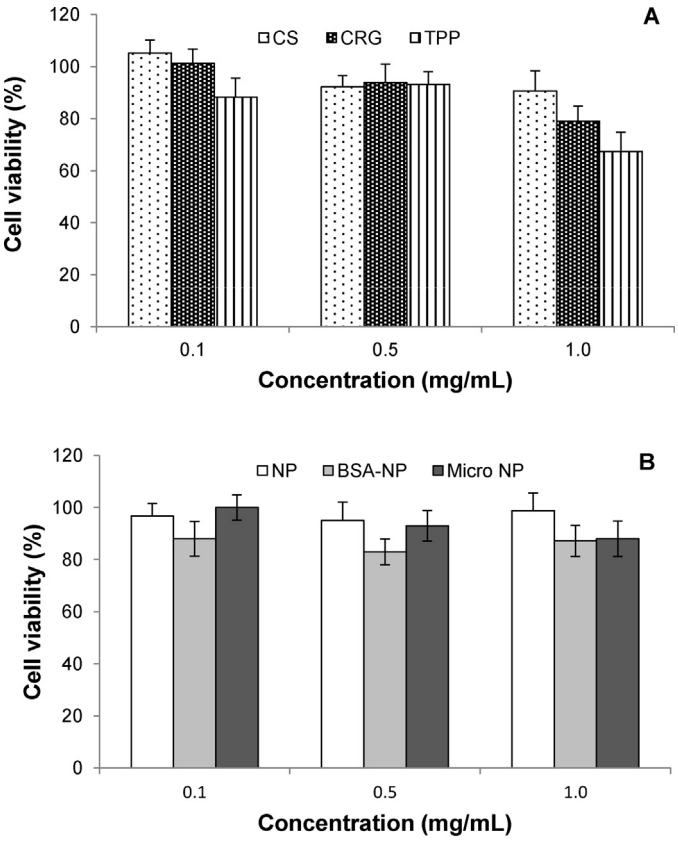

Fig. 4. Calu-3 cells viability measured by the MTT assay after 24 h exposure to raw materials (A – CS: chitosan, CRG: carrageenan, TPP: tripolyphosphate) and nanoparticle-based formulations (B – NP: nanoparticles, BSA-NP: BSA-loaded nanoparticles, micro NP: microencapsulated nanoparticles). Data represent mean ± SEM ($n = 3$, six replicates per experiment at each concentration).

With respect to the formulations, the factorial experiment reveals that only X_1 (type of materials) and the two-way interaction $X_1{}^*X_2$ are statistically significant ($p < 0.05$). Although the lowest viability induced by raw materials was observed for the highest concentration of TPP (1.0 mg/mL, Fig. 4A), cell viability upon contact with CS/CRG/TPP nanoparticles was above 95% in all instances (Fig. 4B), no concentration-dependent effect being observed. In this manner, as a cell viability of 70% is the threshold beyond which a cytotoxic effect is considered to occur according to ISO 10993-5 (ISO, 2009), the observed effects are devoid of physiological relevance. This indicates that Calu-3 cells do not evidence a particular sensitivity to any of the tested samples, either raw materials or nanoparticle-based formulations, at the tested concentrations.

In A549 cells, a balanced FD of the raw materials showed a significant effect for both main factors (X_1 and X_2) and their interaction ($X_1{}^*X_2$). Among raw materials only CRG and TPP show a significant difference between the concentration levels ($p < 0.05$), cell viability decreasing with increasing concentrations, particularly at the concentration of 1 mg/mL (Fig. 5A). Nevertheless, cell viabilities were higher than 70% in all conditions tested for both polymers. The most deleterious effect was observed for chitosan ($p < 0.05$), which induced high cytotoxicity, as was also detected upon 3 h, even at the lower concentration of 0.1 mg/mL.

The different response of both cell lines to CS exposure (in Calu-3 cells no viability decrease was observed) is most probably related

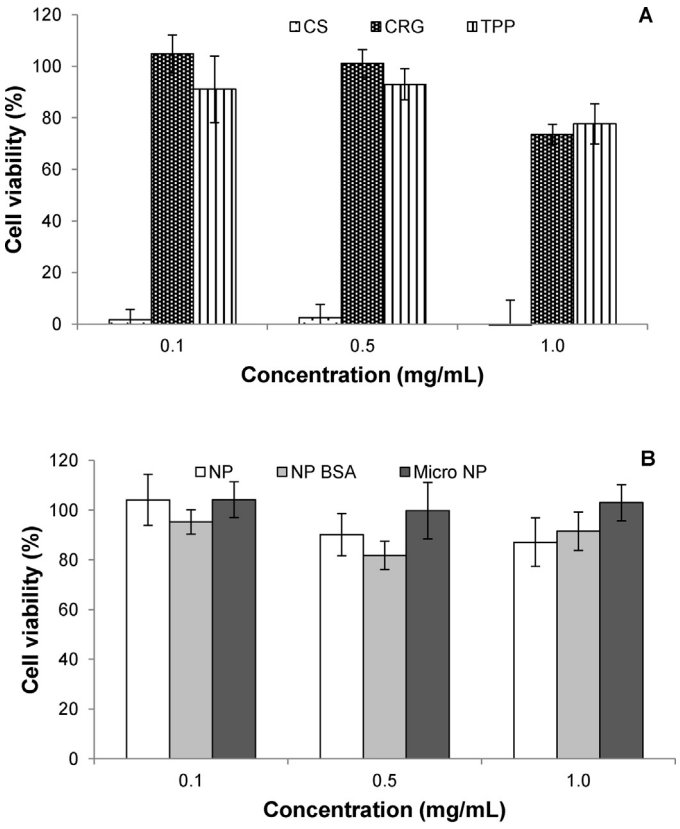

Fig. 5. A549 cells viability measured by the MTT assay after 24 h exposure to raw materials (A – CS: chitosan, CRG: carrageenan, TPP: tripolyphosphate) and nanoparticle-based formulations (B – NP: nanoparticles, BSA-NP: BSA-loaded nanoparticles, micro NP: microencapsulated nanoparticles). Data represent mean ± SEM ($n = 3$, six replicates per experiment at each concentration).

with the different structures evidenced by Calu-3 and A549 cells in culture and with their sensitivity to pH alterations. In fact, while Calu-3 cells are rounder, A549 cells grow according to a more extended profile, as can be easily seen in ATCC webpage (Collection, 2012). Chitosan used in this work is a base and, therefore, is dissolved in acetic acid (pH around 3.2) to assemble the nanoparticles. The same solution was used in the assay, although it was previously diluted with CCM. Upon addition to the cell layer, it was observed on the microscope that A549 cells begin to detach, an effect not perceived for Calu-3 cells. Therefore, the cells are no longer attached to the plate and are easily removed during the washing steps even before the MTT reagent is added, not permitting a reliable measure of the metabolic activity. This indicates that these results should be taken with precaution. Importantly, although there are not many studies testing chitosan solutions in A549 cells, the literature reports an absence of overt toxicity of the polymer in this cell line at concentrations similar to those used in this study, although a different chitosan polymer (regarding molecular weight and salt) was used (Huang, Khor, & Lim, 2004).

The behaviour of A549 cells regarding the tested drug delivery systems was generally similar to that of Calu-3 cells, evidencing a very favourable profile. The statistical details of the FD showed that both main effects (X_1 and X_2) and their interaction ($X_1{}^*X_2$) are significant ($p < 0.05$), the interaction being appreciated in Fig. 5B. Although with slight variations, cell viability was above 80% in all cases. Nevertheless, it is observed that microencapsulated nanoparticles are those causing the more amenable effect.

As a whole, these results indicate that neither the loading of BSA in nanoparticles nor the microencapsulation process induced physiologically relevant alterations on the response of the cells to the

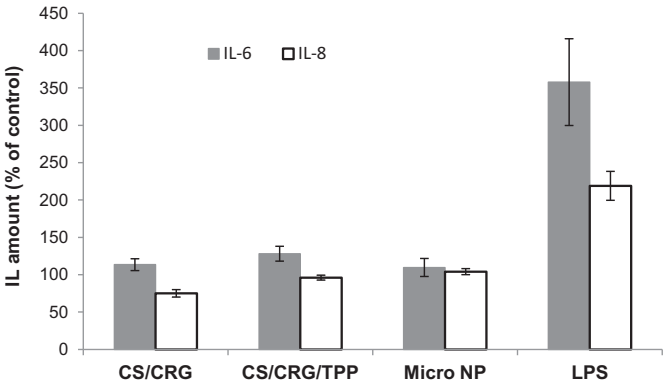

Fig. 6. IL-6 (grey bars) and IL-8 (white bars) secretion by Calu-3 cells exposed for 24 h to CS/CRG and CS/CRG/TPP nanoparticles, microNP and lipopolysaccharide. Data showed as % of release comparing to control (mean ± SD, $n = 3$).

systems. No studies regarding the effect of CS/CRG/TPP nanoparticles on cell viability were reported before, thus hampering the comparison of the present results with others. The most similar studies reported the absence of overt toxicity of either CS/CRG nanoparticles in L929 fibroblasts at the concentration of 1 mg/mL (Grenha et al., 2010) or CS/TPP nanoparticles in Calu-3 and A549 cells (Grenha et al., 2007), while several other formulations of CS-based nanoparticles were also reported to not induce a cytotoxic effect in different cell lines (Caban, Capan, Couvreur, & Dalkara, 2012; Dionísio et al., 2013; Oliveira, Silva, Bitoque, Silva, & Rosa da Costa, 2013).

The findings obtained in this work for all nanoparticle-based formulations in both respiratory cell lines are considered good indicators of biocompatibility. However, the evaluation of a biocompatibility profile demands the use of complementary assays that assess other aspects of cell response, which is certainly of importance to establish a final tendency.

3.5.2. Determination of inflammatory response

In parallel with the evaluation of cell viability, the ability of the carriers to induce an inflammatory response upon contact with the cells has also been used as an indicator of biocompatibility (Lim, Yaacob, Ismail, & Halim, 2010; McCarthy, Inkielewicz-Stępniak, Corbalan, & Radomski, 2012; Mura et al., 2011). The evaluation of such a response might be performed by quantifying the release of inflammatory markers by the cells upon exposure to the drug delivery systems. IL-6 and IL-8 are two cytokines suitable for this end, as IL-6 is responsible for neutrophil activation and IL-8 is a chemotactic agent for inflammatory cells (Lewis & McGee, 1992).

In this assay, the effect of the three nanoparticle-based carriers (CS/CRG/TPP nanoparticles, BSA-loaded nanoparticles and microencapsulated nanoparticles) was evaluated regarding the induction of an inflammatory phenotype in the Calu-3 cells by means of the determination of released IL-6 and IL-8. The obtained results are depicted in Fig. 6. The assessment was conducted upon 24 h exposure to the drug delivery systems (1.0 mg/mL) using LPS as a positive control (10 μg/mL) and CCM as a negative control. The amount of cytokines released in response to CCM was considered 100% and all the other results are presented with respect to that value. As expected, a basal concentration of cytokines in the supernatant was detected in control cells (incubated only with CCM) (Grainger, Greenwell, Martin, & Forbes, 2009; Mura et al., 2011) and IL-8 was secreted at a higher concentration than IL-6 (Mura et al., 2011; Zhu et al., 2010).

Remarkably, no significant effect was elicited by either CS/CRG/TPP nanoparticles or the microencapsulated counterparts as compared with untreated cells. Additionally, IL-8 and IL-6 levels

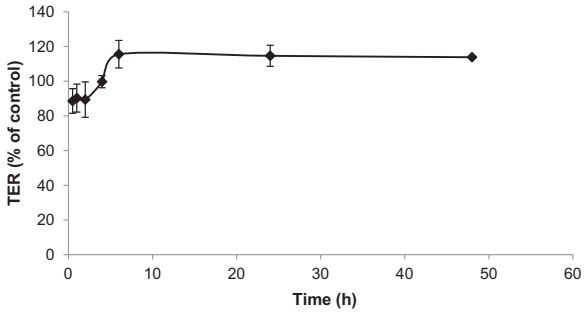

Fig. 7. Transepithelial electrical resistance (TER) of Calu-3 cell layers upon incubation with CS/CRG/TPP nanoparticle suspension (1.0 mg/mL). Data represent mean ± SEM of three experiments ($n = 3$ per experiment).

did not differ between the treatment groups, indicating an absence of effect of the microencapsulation process.

Nanoparticles produced without TPP were also tested as controls, evidencing a response very similar to that of CS/CRG/TPP nanoparticles, which indicates that the inclusion of TPP does not induce a different effect. Finally, a significant increase in the release of both cytokines was only found upon the exposure to LPS (approximately 220% for IL-8 and 360% for IL-6; $p < 0.05$). This effect was expected, as LPS is known to induce an inflammatory response, corresponding to reported findings (Alfaro-Moreno et al., 2009; Mura et al., 2011).

3.5.3. *Evaluation of epithelial integrity*

Intercellular structures are crucial for epithelial development and function. Tight junctions are the most restrictive intercellular junctions, forming a continuous band which completely circumvents the periphery of epithelial cells at the mucosal surface (Matter & Balda, 2003). As mentioned above, and contrary to A549 cells, Calu-3 cells have the ability to form tight junctions *in vitro*, displaying the properties characteristic of an epithelial barrier (Grainger et al., 2006).

In this study, Calu-3 cells were exposed to CS/CRG/TPP nanoparticles at 1 mg/mL to determine the effect of the drug delivery system on the epithelial integrity, as a complementary biocompatibility indicator. The TER was continuously monitored for 48 h and the results are shown in Fig. 7. It is observed that the TER did not suffer significant alterations after treatment with nanoparticles over a period of 48 h. Although not statistically significant, a slight decrease of approximately 10% with respect to control was observed at early time points, but at 4 h the TER reached 100% again and surpassed that value at later times.

No similar results were found on Calu-3 cells, but an increase in TER has been reported in Caco-2 cells (intestinal epithelium) as a response of the cells to an external stimulation (Klingberg, Pedersen, Cencic, & Budde, 2005; Sonnier, Bailey, Pritts, & Lentsch, 2011), in one case being associated with a response to an inflammatory stimulus (Sonnier et al., 2011). Nevertheless, in our study this correlation cannot be established as no significant inflammatory response was obtained upon contact with the nanoparticles, as evidenced above. On the other side, although a decrease in TER was observed in many occasions with chitosan solutions in several epithelial cell lines including the Calu-3 (Florea, Thanou, Junginger, & Borchard, 2006; Portero, Remuñán-López, & Nielsen, 2002; Smith, Wood, & Dornish, 2004), an absence of effect of chitosan-based nanoparticles is also described in the literature (Behrens, Pena, Alonso, & Kissel, 2002; Grenha et al., 2007). Therefore, this observation comprises an extra indication on the biocompatibility of CS/CRG/TPP nanoparticles.

Although the obtained results are good indicators that no deleterious effects are to be expected for short-term contact of the pulmonary or nasal mucosa with the developed nanocarriers, it is important to recall that the effects of a prolonged administration also require attention. In this regard, the rapid mucus turnover in the nasal mucosa certainly prevents nanoparticle accumulation, but that will not be the case in pulmonary delivery, where this concern in unavoidable. The consequences of long-term exposition to particulates are quite unknown (Dombu & Betbeder, 2013), but a retention half-time of approximately 700 days was reported for humans (Oberdörster et al., 2005). With their ability to evade specific defence mechanisms, once in the lung nanoparticles might either accumulate in the lung tissue, causing inflammation that can trigger more severe effects, or they can translocate for extrapulmonary regions, which is also a matter of great concern. This clearly evidences the urgent need of extra studies addressing the raised concerns, which are lacking in the literature. It is of utmost relevance to determine the fate of nanoparticles when in contact with respiratory epithelia, thus enabling an adequate risk assessment and, hopefully, the establishment of nanoparticles in clinic to become a reality.

4. Conclusion

This work demonstrates the suitability of CS/CRG/TPP nanoparticles as carriers for an application in pulmonary and nasal drug delivery, with a particular emphasis on their biocompatibility potential. Apart from the ability to associate a model macromolecule, BSA, the nanoparticles demonstrated to be stable in presence of an amount of lysozyme simulating *in vivo* conditions. The nanocarriers also evidenced stability upon freeze-drying in presence of glucose or sucrose, used as cryoprotectants. The protein-loaded nanoparticles were successfully incorporated in microspheres by means of a spray-drying process, resulting in a dry powder with suitable properties for lung delivery. Moreover, the developed carriers exhibited low or negligible toxicity in contact with two respiratory cell lines representing both the nasal and pulmonary epithelium, as demonstrated by the effects on cell metabolic activity and transepithelial electrical resistance. These findings were reinforced by the observation of no inflammatory response generated upon 24 h of exposure of the cells to the carriers. Altogether, these results are an encouraging indicator of the biocompatibility and safety of CS/CRG/TPP nanoparticles regarding nasal and pulmonary delivery, making them suitable candidates for these applications.

Acknowledgements

This work was supported by National Portuguese funding through FCT – Fundação para a Ciência e a Tecnologia, projects PTDC/SAU-FCF/100291/2008, PTDC/DTP-FTO/0094/2012 and PEst-OE/EQB/LA0023/2013, as well as by the Spanish Government (ISCIII, Acción Estratégica de Salud, PS09/00816). Research of Clara Cordeiro is supported by FCT project PEst-OE/MAT/UI0006/2014. Susana Rodrigues acknowledges her PhD scholarship from FCT (reference SFRH/BD/52426/2013), as well as a ShareBiotech mobility grant.

References

Abdelwahed, W., Degobert, G., Stainmesse, S., & Fessi, H. (2006). Freeze-drying of nanoparticles: Formulation, process and storage considerations. *Advanced Drug Delivery Reviews*, *58*(15), 1688–1713.

Aillon, K. L., Xie, Y., El-Gendy, N., Berkland, C. J., & Forrest, M. L. (2009). Effects of nanomaterial physicochemical properties on in vivo toxicity. *Advanced Drug Delivery Reviews*, *61*(6), 457–466.

Al-Qadi, S., Grenha, A., Carrión-Recio, D., Seijo, B., & Remuñán-López, C. (2012). Microencapsulated chitosan nanoparticles for pulmonary protein delivery: In vivo evaluation of insulin-loaded formulations. *Journal of Controlled Release*, *157*, 383–390.

Alfaro-Moreno, E., Torres, V., Miranda, J., Martínez, L., García-Cuellar, C., Nawrot, T. S., et al. (2009). Induction of IL-6 and inhibition of IL-8 secretion in the human airway cell line Calu-3 by urban particulate matter collected with a modified method of PM sampling. *Environmental Research*, *109*(5), 528–535.

Behrens, I., Pena, A. I., Alonso, M. J., & Kissel, T. (2002). Comparative uptake studies of bioadhesive and non-bioadhesive nanoparticles in human intestinal cell lines and rats: The effect of mucus on particle adsorption and transport. *Pharmaceutical Research*, *19*, 1185–1193.

Beirowski, J., Inghelbrecht, S., Arien, A., & Gieseler, H. (2011). Freeze drying of nanosuspensions, 2: The role of the critical formulation temperature on stability of drug nanosuspensions and its practical implication on process design. *Journal of Pharmaceutical Sciences*, *100*, 4471–4481.

Beirowski, J., Inghelbrecht, S., Arien, A., & Gieseler, H. (2012). Freeze drying of nanosuspensions, Part 3: Investigation of factors compromising storage stability of highly concentrated drug nanosuspensions. *Journal of Pharmaceutical Sciences*, *101*, 354–362.

Bernkop-Schnürch, A., Weithaler, A., Albrecht, K., & Greimel, A. (2006). Thiomers: Preparation and in vitro evaluation of a mucoadhesive nanoparticulate drug delivery system. *International Journal of Pharmaceutics*, *317*(1), 76–81.

Bogataj, M., Vovk, T., Kerec, M., Dimnik, A., Grabnar, I., & Mrhar, A. (2003). The correlation between zeta potential and mucoadhesion strength on pig vesical mucosa. *Biological and Pharmaceutical Bulletin*, *26*(5), 743–746.

Bosquillon, C., Lombry, C., Préat, V., & Vanbever, R. (2001). Influence of formulation excipients and physical characteristics of inhalation dry powders on their aerosolization performance. *Journal of Controlled Release*, *70*(3), 329–339.

Caban, S., Capan, Y., Couvreur, P., & Dalkara, T. (2012). Preparation and characterization of biocompatible chitosan nanoparticles for targeted brain delivery of peptides. In S. Skaper (Ed.), *Neurotrophic Factors* (pp. 321–332). London: Humana Press.

Carmichael, J., DeGraff, W., Gazdar, A., Minna, J., & Mitchell, J. (1987). Evaluation of a tetrazolium-based semiautomated colorimetric assay: Assessment of chemosensitivity testing. *Cancer Research*, *47*, 936–942.

Carvalho, E. L. S., Grenha, A., Remunan-Lopez, C., Alonso, M. J., & Seijo, B. (2009). Mucosal delivery of liposome-chitosan nanoparticle complexes. *Methods in Enzymology Liposomes, Pt G*, *465*, 289–312.

Carvalho, F., Bruschi, M., Evangelista, R., & Gremião, M. (2010). Mucoadhesive drug delivery systems. *Brazilian Journal of Pharmaceutical Sciences*, *46*(1), 1–17.

Casettari, L., Vllasaliu, D., Mantovani, G., Howdle, S. M., Stolnik, S., & Illum, L. (2010). Effect of PEGylation on the toxicity and permeability enhancement of chitosan. *Biomacromolecules*, *11*(11), 2854–2865.

Chacón, M., Molpeceres, J., Berges, L., Guzmán, M., & Aberturas, M. R. (1999). Stability and freeze-drying of cyclosporine loaded poly(D,L lactide–glycolide) carriers. *European Journal of Pharmaceutical Sciences*, *8*(2), 99–107.

Collection, A. T. C. (2012). A549 (ATCC® CCL-185™).

de la Fuente, M., Seijo, B., & Alonso, M. J. (2008). Novel hyaluronan-based nanocarriers for transmucosal delivery of macromolecules. *Macromolecular Bioscience*, *8*(5), 441–450.

Desai, M. P., Labhasetwar, V., Amidon, G. L., & Levy, R. J. (1996). Gastrointestinal uptake of biodegradable microparticles: Effect of particle size. *Pharmaceutical Research*, *13*(12), 1838–1845.

Dionísio, M., Cordeiro, C., Remuñán-López, C., Seijo, B., Rosa da Costa, A., & Grenha, A. (2013). Pullulan-based nanoparticles as carriers for transmucosal protein delivery. *European Journal of Pharmaceutical Sciences*, *50*, 102–113.

Dombu, C. Y., & Betbeder, D. (2013). Airway delivery of peptides and proteins using nanoparticles. *Biomaterials*, *34*(2), 516–525.

Du, H., Cai, X., & Zhai, G. (2014). Advances in the targeting molecules modified chitosan-based nanoformulations. *Current Drug Targets*, *14*(9), 1034–1052.

El-Gibaly, I. (2002). Development and in vitro evaluation of novel floating chitosan microcapsules for oral use: Comparison with non-floating chitosan microspheres. *International Journal of Pharmaceutics*, *249*(1–2), 7–21.

Florea, B. I., Thanou, M., Junginger, H. E., & Borchard, G. (2006). Enhancement of bronchial octreotide absorption by chitosan and N-trimethyl chitosan shows linear in vitro/in vivo correlation. *Journal of Controlled Release*, *110*(2), 353–361.

Forbes, B., & Ehrhardt, C. (2005). Human respiratory epithelial cell culture for drug delivery applications. *European Journal of Pharmaceutics and Biopharmaceutics*, *60*(2), 193–205.

Foster, K. A., Avery, M. L., Yazdanian, M., & Audus, K. L. (2000). Characterization of the Calu-3 cell line as a tool to screen pulmonary drug delivery. *International Journal of Pharmaceutics*, *208*(1–2), 1–11.

Foster, K. A., Yazdanian, M., & Audus, K. L. (2001). Microparticulate uptake mechanisms of in-vitro cell culture models of the respiratory epithelium. *Journal of Pharmacy and Pharmacology*, *53*(1), 57–66.

Freixeiro, P., Diéguez-Casal, E., Costoya, L., Seijo, B., Ferreirós, C. M., Criado, M. T., et al. (2013). Study of the stability of proteoliposomes as vehicles for vaccines against *Neisseria meningitidis* based on recombinant porin complexes. *International Journal of Pharmaceutics*, *443*(1–2), 1–8.

Gaspar, R., & Duncan, R. (2009). Polymeric carriers: Preclinical safety and the regulatory implications for design and development of polymer therapeutics. *Advanced Drug Delivery Reviews*, *61*(13), 1220–1231.

Goycoolea, F. M., Lollo, G., Remunan-Lopez, C., Quaglia, F., & Alonso, M. J. (2009). Chitosan-alginate blended nanoparticles as carriers for the transmucosal delivery of macromolecules. *Biomacromolecules*, *10*(7), 1736–1743.

Grainger, C., Greenwell, L., Lockley, D., Martin, G., & Forbes, B. (2006). Culture of Calu-3 cells at the air interface provides a representative model of the airway epithelial barrier. *Pharmaceutical Research*, *23*(7), 1482–1490.

Grainger, C. I., Greenwell, L. L., Martin, G. P., & Forbes, B. (2009). The permeability of large molecular weight solutes following particle delivery to air-interfaced cells that model the respiratory mucosa. *European Journal of Pharmaceutics and Biopharmaceutics*, *71*(2), 318–324.

Grenha, A. (2012). Chitosan nanoparticles: A survey of preparation methods. *Journal of Drug Targeting*, *20*(4), 291–300.

Grenha, A., Gomes, M. E., Rodrigues, M., Santo, V. E., Mano, J. F., Neves, N. M., et al. (2010). Development of new chitosan/carrageenan nanoparticles for drug delivery applications. *Journal of Biomedical Materials Research A*, *92A*(4), 1265–1272.

Grenha, A., Grainger, C. I., Dailey, L. A., Seijo, B., Martin, G. P., Remuñán-López, C., et al. (2007). Chitosan nanoparticles are compatible with respiratory epithelial cells in vitro. *European Journal of Pharmaceutical Sciences*, *31*(2), 73–84.

Grenha, A., Seijo, B., & Remuñán-López, C. (2005). Microencapsulated chitosan nanoparticles for lung protein delivery. *European Journal of Pharmaceutical Sciences*, *25*, 427–437.

Gupta, H., & Sharma, A. (2009). Recent trends in protein and peptide drug delivery systems. *Asian Journal of Pharmaceutics*, *3*, 69–75.

Hirsjärvi, S., Peltonen, L., & Hirvonen, J. (2009). Effect of sugars, surfactant, and tangential flow filtration on the freeze-drying of poly(lactic acid) nanoparticles. *AAPS PharmSciTech*, *10*(2), 488–494.

Hoppentocht, M., Hagedoorn, P., Frijlink, H. W., & de Boer, A. H. (2014). Developments and strategies for inhaled antibiotic drugs in tuberculosis therapy: A critical evaluation. *European Journal of Pharmaceutics and Biopharmaceutics*, *86*(1), 23–30.

Huang, M., Khor, E., & Lim, L.-Y. (2004). Uptake and cytotoxicity of chitosan molecules and nanoparticles: Effects of molecular weight and degree of deacetylation. *Pharmaceutical Research*, *21*(2), 344–353.

ISO. (2009). Biological evaluation of medical devices Part 5: Tests for in vitro cytotoxicity. In *I. O. f. Standardization 10993-5*.

Jani, P., Halbert, G., Langridge, J., & Florence, A. (1990). Nanoparticle uptake by the rat gastrointestinal mucosa: Quantitation and particle size dependency. *Journal of Pharmacy and Pharmacology*, *42*(12), 821–826.

Klingberg, T. D., Pedersen, M. H., Cencic, A., & Budde, B. B. (2005). Application of measurements of transepithelial electrical resistance of intestinal epithelial cell monolayers to evaluate probiotic activity. *Applied and Environmental Microbiology*, *71*(11), 7528–7530.

Konstan, M., Chen, P., Sherman, J., Thomassen, M., Woodm, R., & Boat, T. (1981). Human lung lysozyme: Sources and properties. *American Reviews of Respiratory Disease*, *123*, 120–124.

Kumar, G., Shafiq, N., & Malhotra, S. (2012). Drug-loaded PLGA nanoparticles for oral administration: Fundamental issues and challenges ahead. *Critical Reviews in Therapeutic Drug Carrier Systems*, *29*(2), 149–182.

Labiris, N., Holbrook, A., Chrystyn, H., Macleod, S., & Newhouse, M. (1999). Dry powder versus intravenous and nebulized gentamicin in cystic fibrosis and bronchiectasis. *American Journal of Respiratory and Critical Care Medicine*, *160*, 1711–1716.

Lehr, C.-M., Bouwstra, J. A., Schacht, E. H., & Junginger, H. E. (1992). In vitro evaluation of mucoadhesive properties of chitosan and some other natural polymers. *International Journal of Pharmaceutics*, *78*, 43–48.

Lewis, C., & McGee, J. D. (1992). *The macrophage*. Oxford: IRL Press.

Li, S., Patapoff, T., Overcashier, D., Hsu, C., Nguyen, T., & Borchardt, R. (1996). Effects of reducing sugars on the chemical stability of human relaxin in the lyophilized state. *Journal of Pharmaceutical Sciences*, *85*(8), 873–877.

Li, Y.-Z., Sun, X., Gong, T., Liu, J., Zuo, J., & Zhang, Z.-R. (2010). Inhalable microparticles as carriers for pulmonary delivery of thymopentin-loaded solid lipid nanoparticles. *Pharmaceutical Research*, *27*(9), 1977–1986.

Lim, C. K., Yaacob, N. S., Ismail, Z., & Halim, A. S. (2010). In vitro biocompatibility of chitosan porous skin regenerating templates (PSRTs) using primary human skin keratinocytes. *Toxicology in Vitro*, *24*(3), 721–727.

Malafaya, P., Silva, G., & Reis, R. (2007). Natural-origin polymers as carriers and scaffolds for biomolecules and cell delivery in tissue engineering application. *Advanced Drug Delivery Reviews*, *59*, 207–233.

Marttin, E., Schipper, N. G. M., Verhoef, J. C., & Merkus, F. W. H. M. (1998). Nasal mucociliary clearance as a factor in nasal drug delivery. *Advanced Drug Delivery Reviews*, *29*(1–2), 13–38.

Matter, K., & Balda, M. (2003). Functional analysis of tight junctions. *Methods*, *30*, 228–234.

McCarthy, J., Inkielewicz-Stępniak, I., Corbalan, J. J., & Radomski, M. W. (2012). Mechanisms of toxicity of amorphous silica nanoparticles on human lung submucosal cells in vitro: Protective effects of fisetin. *Chemical Research in Toxicology*, *25*(10), 2227–2235.

Mura, S., Hillaireau, H., Nicolas, J., Le Droumaguet, B., Gueutin, C., Zanna, S., et al. (2011). Influence of surface charge on the potential toxicity of PLGA nanoparticles towards Calu-3 cells. *International Journal of Nanomedicine*, *6*, 2591–2605.

Muzzarelli, R. (1997). Human enzymatic activities related to the therapeutic administration of chitin derivatives. *Cellular and Molecular Life Sciences*, *53*, 131–140.

Nahar, K., Gupta, N., Gauvin, R., Absar, S., Patel, B., Gupta, V., et al. (2013). In vitro, in vivo and ex vivo models for studying particle deposition and drug absorption of inhaled pharmaceuticals. *European Journal of Pharmaceutical Sciences*, *49*(5), 805–818.

Oberdörster, G., Oberdörster, E., & Oberdörster, J. (2005). Nanotoxicology: An emerging discipline evolving from studies of ultrafine particles. *Environmental and Health Perspectives*, *113*, 823–839.

Oliveira, A., Silva, A., Bitoque, D., Silva, G., & Rosa da Costa, A. (2013). Transfection efficiency of chitosan and thiolated chitosan in retinal pigment epithelium cells: A comparative study. *Journal of Pharmacy and Bioallied Sciences*, *5*, 111–118.

Oyarzun-Ampuero, F., Brea, J., Loza, M., Torres, D., & Alonso, M. J. (2009). Chitosan-hyaluronic acid nanoparticles loaded with heparin for the treatment of asthma. *International Journal of Pharmaceutics*, *381*, 122–129.

Pinto Reis, C., Neufeld, R., Ribeiro, A., & Veiga, F. (2006). Nanoencapsulation II. Biomedical applications and current status of peptide and protein nanoparticulate delivery systems. *Nanomedicine: Nanotechnology, Biology, and Medicine*, *2*, 53–65.

Portero, A., Remuñán-López, C., & Nielsen, H. M. (2002). The potential of chitosan in enhancing peptide and protein absorption across the TR146 cell culture model — An in vitro model of the buccal epithelium. *Pharmaceutical Research*, *19*(2), 169–174.

Pourshahab, P. S., Gilani, K., Moazeni, E., Eslahi, H., Fazeli, M. R., & Jamalifar, H. (2011). Preparation and characterization of spray dried inhalable powders containing chitosan nanoparticles for pulmonary delivery of isoniazid. *Journal of Microencapsulation*, *28*(7), 605–613.

Rodrigues, S., Dionísio, M., Remuñán-López, C., & Grenha, A. (2012). Biocompatibility of chitosan carriers with application in drug delivery. *Journal of Functional Biomaterials*, *3*, 615–641.

Rodrigues, S., Rosa da Costa, A., & Grenha, A. (2012). Chitosan/carrageenan nanoparticles: Effect of cross-linking with tripolyphosphate and charge ratios. *Carbohydrate Polymers*, *89*, 282–289.

Rogueda, P., & Traini, D. (2007). The nanoscale in pulmonary delivery. Part 1: Deposition, fate, toxicology and effects. *Expert Opinion on Drug Delivery*, *4*(6), 595–606.

Sameti, M., Bohr, G., Ravi Kumar, M. N. V., Kneuer, C., Bakowsky, U., Nacken, M., et al. (2003). Stabilisation by freeze-drying of cationically modified silica nanoparticles for gene delivery. *International Journal of Pharmaceutics*, *266*(1–2), 51–60.

Sandri, G., Bonferoni, M., Rossi, S., Ferrari, F., Boselli, C., & Caramella, C. (2010). Insulin-loaded nanoparticles based on N-trimethyl chitosan: In vitro (Caco-2 model) and ex vivo (excised rat jejunum, duodenum, and ileum) evaluation of penetration enhancement properties. *AAPS PharmSciTech*, *11*(1), 362–371.

Scherließ, R. (2011). The MTT assay as tool to evaluate and compare excipient toxicity in vitro on respiratory epithelial cells. *International Journal of Pharmaceutics*, *411*(1–2), 98–105.

Smith, J., Wood, E., & Dornish, M. (2004). Effect of chitosan on epithelial cell tight junctions. *Pharmaceutical Research*, *21*(1), 43–49.

Sonnier, D. I., Bailey, S. R., Pritts, T. A., & Lentsch, A. B. (2011). TNF-α induced vectorial secretion of IL-8 corresponds to development of transepithelial electrical resistance in Caco-2 cells. *Gastroenterology*, *140*(5), S–S1044.

Sung, J. C., Pulliam, B. L., & Edwards, D. A. (2007). Nanoparticles for drug delivery to the lungs. *Trends in Biotechnology*, *25*(12), 563–570.

Umrethia, M., Kett, V. L., Andrews, G. P., Malcolm, R. K., & Woolfson, A. D. (2010). Selection of an analytical method for evaluating bovine serum albumin concentrations in pharmaceutical polymeric formulations. *Journal of Pharmaceutical and Biomedical Analysis*, *51*(5), 1175–1179.

Vauthier, C., & Bouchemal, K. (2009). Methods for the preparation and manufacture of polymeric nanoparticles. *Pharmaceutical Research*, *26*(5), 1025–1058.

Vila, A., Sánchez, A., Tobío, M., Calvo, P., & Alonso, M. J. (2002). Design of biodegradable particles for protein delivery. *Journal of Controlled Release*, *78*(1–3), 15–24.

Wang, W. (2000). Lyophilization and development of solid protein pharmaceuticals. *International Journal of Pharmaceutics*, *203*(1–2), 1–60.

Williams, D. F. (2008). On the mechanisms of biocompatibility. *Biomaterials*, *29*(20), 2941–2953.

Winton, H., Wan, H., Cannell, M., Gruenert, D., Thompson, P., Garrod, D., et al. (1998). Cell lines of pulmonary and non-pulmonary origin as tools to study the effects of house dust mite proteinases on the regulation of epithelial permeability. *Clinical & Experimental Allergy*, *28*(10), 1273–1285.

Wu, L., Zhang, J., & Watanabe, W. (2011). Physical and chemical stability of drug nanoparticles. *Advanced Drug Delivery Reviews*, *63*(6), 456–469.

Zhu, Y., Chidekel, A., & Shaffer, T. (2010). Cultured human airway epithelial cells (Calu-3): A model of human respiratory function, structure, and inflammatory responses. *Critical Care Research and Practice*, *2010*, 1–8.

Zorzi, G. K., Párraga, J. E., Seijo, B., & Sánchez, A. (2011). Hybrid nanoparticle design based on cationized gelatin and the polyanions dextran sulfate and chondroitin sulfate for ocular gene therapy. *Macromolecular Bioscience*, *11*(7), 905–913.